Open Access Full Text Article

ORIGINAL RESEARCH

Disrupted Balance of Short- and Long-Range Functional Connectivity Density in Patients with Herpes Zoster or Postherpetic Neuralgia: A Resting-State fMRI Study

Jian Jiang[1,2,*], Xiaoyan Hou[1,*], Lili Gu[3], Xian Liu [ID][1], Huiting Lv[1], Jiaxin Xiong[1], Hongmei Kuang[1,2], Xiaofeng Jiang[1], Shunda Hong[1,2]

[1]Department of Radiology, The First Affiliated Hospital, Nanchang University, Nanchang, People's Republic of China; [2]Jiangxi Medical Imaging Research Institute, Nanchang, People's Republic of China; [3]Department of Pain, The First Affiliated Hospital, Nanchang University, Nanchang, People's Republic of China

*These authors contributed equally to this work

Correspondence: Shunda Hong, Department of Radiology, The First Affiliated Hospital, Nanchang University, 17 Yongwaizheng Street, Nanchang, Jiangxi, 330006, People's Republic of China, Tel/Fax +86-791-88693825, Email dyfy05441@ncu.edu.cn

Purpose: This study aimed to explore the abnormal changes in short- and long-range functional connectivity density (FCD) in patients with herpes zoster (HZ) and postherpetic neuralgia (PHN).

Patients and Methods: Twenty HZ patients, 22 PHN patients, and 19 well-matched healthy controls (HCs) underwent resting-state functional magnetic resonance imaging scans. We used FCD mapping, a data-driven graph theory method, to investigate local and global functional connectivity patterns. Both short- and long-range FCD were calculated and compared among the PHN, HZ, and HC groups. Then, the abnormal regions were used to calculate seed-based functional connectivity. Finally, correlation analyses were performed between the altered FCD values and clinical datas.

Results: Compared with HCs, HZ patients showed significantly increased long-range FCD of the bilateral cerebellum, thalamus, parahippocampal gyrus, superior temporal gyrus and lingual gyrus. HZ patients also displayed significantly decreased short-range FCD of the bilateral posterior cingulate gyrus, median cingulate/paracingulate gyri, and left precuneus. Compared with HCs, PHN patients displayed significantly decreased long-range FCD of the bilateral superior frontal gyrus and decreased short-range FCD in the bilateral posterior cingulate gyrus, median cingulate/paracingulate gyri, and precuneus. However, there was no significant difference in either long-range or short-range FCD between the PHN and HZ patients. Long-range FCD deficit areas and the right insula showed altered functional connectivity in PHN patients. Furthermore, pain duration in patients with PHN was correlated with abnormal long-range FCD.

Conclusion: Herpes zoster pain widely affects intra- and inter-regional functional connectivity, leading to disrupted short-range FCD and increased long-range FCD during different stages of the disease. Long-term chronic pain in PHN patients may impair the pain emotion regulation pathway. These findings could improve our understanding of the pathophysiological mechanisms of HZ and PHN and offer neuroimaging markers for HZ and PHN.

Keywords: functional connectivity density, herpes zoster, postherpetic neuralgia, pain, functional magnetic resonance imaging

Introduction

Herpes zoster (HZ; also known as shingles) — a skin disease caused by reactivation of the varicella-zoster virus (VZV) — is commonly accompanied by acute pain and erythematous rash.[1] Postherpetic neuralgia (PHN) is a chronic neuropathic pain syndrome that persists or develops after the rash has healed and is the most common complication of HZ, occurring in 5%–30% of patients.[2,3] PHN is defined as experiencing typical chronic neuropathic pain that lasts for

2753

more than a month after the resolution of HZ and is associated with various peripheral and central nervous system abnormalities.[4] Debilitating and refractory pain seriously affects patients' mental and physical health. Although antiviral medications combined with steroids may reduce the risk of PHN, they are most effective shortly after rash onset.[3] Such timely treatment requires a quick diagnosis in the early stage of HZ. Currently, HZ and PHN are difficult to diagnose in clinical practice.[3] Therefore, it is crucial to identify other complementary diagnostic methods.

Identifying specific neuroimaging markers of shingles and exploring its internal pathophysiological mechanism can facilitate the early diagnosis of HZ and PHN. Functional magnetic resonance imaging (fMRI) is an effective technique widely used to identify specific neuronal imaging markers. Recently, numerous neuroimaging studies have confirmed the changes in brain function in patients with HZ and PHN. Regional homogeneity (ReHo) and the amplitude of low-frequency fluctuations (ALFF), indices commonly used to explore neuronal activity in the brain, have exhibited abnormal values in the pain matrix (eg, frontal lobe, insula, and cerebellum) as well as in the brainstem and parietal lobe in HZ and PHN patients.[5] These fMRI studies have confirmed the close association between the pathophysiology of PHN and functional abnormalities in local brain regions,[5] however, they have limitations in evaluating the functional interactions or integration among different brain regions. Resting-state functional connectivity (rsFC) is a method that measures temporal correlations of blood oxygenation level-dependent (BOLD) signal fluctuations and has been widely used to study the interactions between different brain regions.[6] For example, PHN patients were found to have reduced rsFC among the dorsolateral prefrontal cortex, anterior cingulate cortex, and posterior cingulate cortex. This reduction leads to weakened functional integration and disrupted intrinsic connectivity, between these regions and the default mode network.[6]

However, to date, there have been few advanced studies on whole-brain functional connectivity changes in HZ and PHN patients. Functional connectivity density (FCD) mapping is a voxel-level, data-driven graph theory method that measures the number of functional connections between a given voxel and other voxels, with higher FCD values indicating that these voxels are functionally connected to a large number of other brain voxels and play a more vital role in information processing.[7] According to the neighborhood relationship between brain voxels, FCD can be further divided into short- and long-range FCD,[8] which can simultaneously capture spontaneous neuronal activity and connectivity within and between regions, in contrast to ReHo. Unlike traditional seed-based rsFC analysis,[9] FCD does not require a priori selection of seed regions, thereby avoiding subjective bias.

In a previous study by our research group, FCD was used to explore intrinsic functional connectivity in HZ and PHN patients, and it was found that both HZ and PHN patients exhibited damage to the default mode network.[10] However, it is still unclear whether this damage is related to the disruption of connectivity among adjacent structures or more distant damage. Therefore, this study aimed to further explore the differences in long-range FCD and short-range FCD throughout the whole brain in HZ and PHN patients. We evaluated alterations in local and global functional connectivity patterns in patients with HZ and PHN. Short-range FCD reflects the plasticity of functional connections around voxels, while long-range FCD can reflect the plasticity of remote functional connections.[11] This approach measures significant local and global functional connections of voxels over the whole brain, is suitable for investigating altered intrinsic functional connectivity, and provides complementary information for more targeted analysis.

The main objectives of this study were as follows: (i) to evaluate alterations in the long- and short-range FCD in patients with HZ and PHN and (ii) to correlate changes in FC with clinical variables such as pain intensity and duration and establish a link between FC changes and clinical data to provide further imaging evidence of the central nervous system mechanisms underlying PHN and HZ.

Materials and Methods
Participants

The study recruited 20 patients with HZ (age: 58.6±10.3 years, 13 males/7 females) and 22 patients with PHN (63.1±10.9 years, 11 males/11 females) from the Pain Department of the First Affiliated Hospital of Nanchang University, along with 19 sex- and age-matched healthy controls (HCs) (57.6±7.3 years, 9 males/11 females). All participants were right-handed. The clinical diagnosis of HZ or PHN was made by two experienced pain doctors based on the standards of the International Association for

the Study of Pain (IASP).[12] All patients underwent MRI scans on the day of admission and before systemic treatment. Before fMRI scanning, the visual analog scale (VAS) was used to assess the intensity of spontaneous pain in HZ and PHN patients. Patients were required to have a VAS score ≥5 (moderate to severe pain) to be included in this study, in this scale, pain intensity is indicated on a scale from 0 to 10, with 0 indicating no pain and 10 indicating the most severe unbearable pain. Psychological examinations, including the Symptom Checklist 90 (SCL-90), Hamilton Anxiety Scale (HAMA), and Hamilton Depression Scale (HAMD), were also completed to assess the emotional state of the patients. All patients were included according to the following criteria: (I) VAS score ≥5; (II) right-handedness; (III) clinically confirmed PHN and HZ. All HCs complied with the following standards: (I) sex- and age-matched, and (II) VAS score=0. None of the participants had a history of mental or neurological disorders, alcoholism, drug abuse, other types of pain, or drug use that could affect brain activity. The inclusion and exclusion criteria for the study participants are presented as a flowchart in the Supplementary Material. This study followed the principles of the Declaration of Helsinki and was approved by the Medical Research Ethics Committee and Institutional Review Board of the First Affiliated Hospital of Nanchang University (ethics approval code: 20200145). Written informed consent was obtained from all the participants.

MRI Data Acquisition

Functional magnetic resonance imaging data for all participants were obtained using a Trio 3.0T MRI scanner (Siemens, Germany) at the Department of Radiology, First Affiliated Hospital of Nanchang University. First, all participants underwent routine brain MRI scans to exclude organic brain lesions. Second, high-resolution 3D-T1 sequence scans were performed to obtain a high-resolution three-dimensional anatomical image, with 176 sagittal T1-weighted images (repetition time [TR]=1900 ms, echo time [TE]=2.26 ms, flip angle=9°, matrix=240×256, field of view [FOV]=215×230 mm, slice thickness=1.0 mm, scan time=8 min). Finally, 240 functional images were obtained using a single-shot gradient echo-planar imaging sequence (TR=2000 ms, TE=30 ms, flip angle=90°, matrix=64×64, FOV=220×220 mm, slice thickness=4 mm, 30 interleaved axial slices). During the rs-fMRI scan, the participants lay supine on the scanning table, with their heads fixed in place with foam pads to minimize head movement. Headphones were provided to reduce the noise generated by the gradient magnetic field. Participants were instructed to remain as still as possible, close their eyes, and stay awake.

MRI Data Preprocessing

The functional magnetic resonance imaging data were preprocessed using the rs-fMRI data processing assistant (SeeCAT; https://www.nitrc.org/projects/seecat/) toolkit based on the MATLAB2018b (MathWorks, Natick, MA, USA) platform. Data preprocessing included the following steps. 1)Removal of the first 10 time points. 2) Slice timing correction. 3) Head motion correction. Participants with a maximum head translation of >3 mm or head rotation of >3° in the x-, y-, or z-direction were excluded. Next, framewise displacement (FD) was used as a measure of minor head motion in the participants, and those with FD>0.3 were excluded. 4) Linear transformation was used to register the high-resolution T1-weighted structural image with the functional image, which was registered to the standard space of the Montreal Neurological Institute (MNI) (resampling voxel size 3×3×3). 5) Linear regression was employed to eliminate the influence of covariates (Friston 24 head motion parameters, global signal, white matter signal and cerebrospinal fluid signal). 6) Finally, bandpass filtering (0.01–0.1 Hz) and linear drift removal were performed.

FCD Data Preprocessing

Short-range and whole-brain FCD maps of each patient were calculated. The basic principle of FCD is to calculate the *Pearson* correlation coefficient of BOLD signal time series between voxels. Long-range and short-range FCD calculations were performed using the SeeCAT toolbox (http://www.nitrc.org/Projects/seecat/). The detailed steps used to calculate short- and long-range FCD values have been described in previous studies.[7] First, we used a correlation threshold of r>0.25 to screens the functional connectivity between given voxels and other voxels in the whole brain.[10] Second, according to the neighborhood relationship between brain voxels, FCD can be divided into short- or long-range FCD. Following a previous study,[13] we considered connections within a given anatomical distance of 75 mm to be effective regional functional connections (short-range FCD) and functional connections outside this region to be long-

range (long-range FCD; the difference between whole-brain FCD and short-range FCD). Then, the long-range and short-range FCD maps were converted to *Z* scores to improve normality, and finally, the FCD data were spatially smoothed with a 6×6×6 mm³ full-width at half maximum Gaussian kernel.

Region-of-Interest-Based FC Calculation

Regions with significant differences in long-range FCD were set as regions of interest (ROIs) for seed-based rsFC analysis. This was done to study changes in rsFC between the ROI and the whole brain. The DPABI toolbox was utilized to extract the average time course of each ROI (http://rfmri.org/DPARSF). The Pearson correlation coefficient was used to calculate the correlation of the average time course. The r value of FC was transformed into a z value via Fisher's r-to-z transformation to improve the normality of the distribution.

Statistical Analysis

First, the spatial distribution of average short-range and long-range FCD in the HZ, PHN, and HC groups was calculated. Next, an analysis of covariance (ANCOVA) was performed using the DPABI toolbox to examine the differences in FCD among the three groups, with age, sex, and average FD as covariates. GRF correction was employed to reduce the false-positive rate (voxel-level P value< 0.01, cluster-level P value< 0.05). Cohen's d[14] was used as an effect size (ES) indicator of significant differences in the average short- and long-range FCD values of brain areas among groups. The FCD values of the regions with significant differences within the groups were extracted, and a partial correlation analysis was performed on the short- and long-range FCD values and clinical data in the patient groups, with age and sex as covariates. Second, after a random effects single-sample *t*-test in DPABI, we used only FC values for between-group comparisons when the FC values extracted from the ROI analysis between the groups were statistically significant within each group. Then, the z values of all ROIs among groups were evaluated using a general linear model (GLM) analysis in DPABI after controlling for age and sex with GRF correction (voxel-level P value< 0.01, cluster-level P value< 0.05). Cohen's d was used to estimate ES and determine the magnitude of significant differences among the groups. Finally, we evaluated the partial correlation between values of ROI-based rsFC and clinical parameters).

Results
Demographic Characteristics and Clinical Data

Table 1 lists the clinical characteristics of HZ and PHN patients. There were no significant differences in age (HZ vs HC, PHN vs HC, and PHN vs HZ: P = 0.73, 0.07, and 0.18, respectively; two-sample *t*-test) or sex (HZ vs HC, PHN vs HC, and PHN vs HZ: P=0.56, 0.87, and 0.60, respectively; chi-square test) among the three groups. There were significant differences in pain duration, HAMA scores, and HAMD scores between HZ and PHN patients (P<0.05, two-sample *t*-test).

Table 1 Participants' Information

Clinical Information	HZ Patients (n=20)	PHN Patients (n=22)	HC (n=19)	P value
Age (years, mean ± SD)	58.6±10.3	63.1±10.9	57.6±7.3	0.46
Gender (male/female)	13/7	11/11	9/10	0.35
VAS score (mean ± SD)	6.6±0.9	6.3±1.0	–	0.26
Pain duration (days, mean ± SD)	11.9±6.1	85.5±6.2	–	<0.01
SCL-90 (mean ± SD)	123.3±14.3	155.6±47.6	-	0.08
HAMA (mean ± SD)	13.7±6.5	20.1±8.9	-	0.01
HAMD (mean ± SD)	14.2±5.0	21.9±9.2	-	0.01

Abbreviations: HZ, herpes zoster; PHN, postherpetic neuralgia; VAS, visual analog scale; SCL-90, Symptom Checklist 90; HAMA, Hamilton Anxiety Scale; HAMD, Hamilton Depression Scale.

Spatial Distribution of Short-Range and Long-Range FCD in the HZ, PHN and HC Groups

All three groups showed similar spatial distributions of the FCD (Figure 1). The temporal lobe, parietal lobe, limbic lobe, and cingulate lobe revealed a wide distribution of long-range FCD and short-range FCD. In addition, short-range FCD
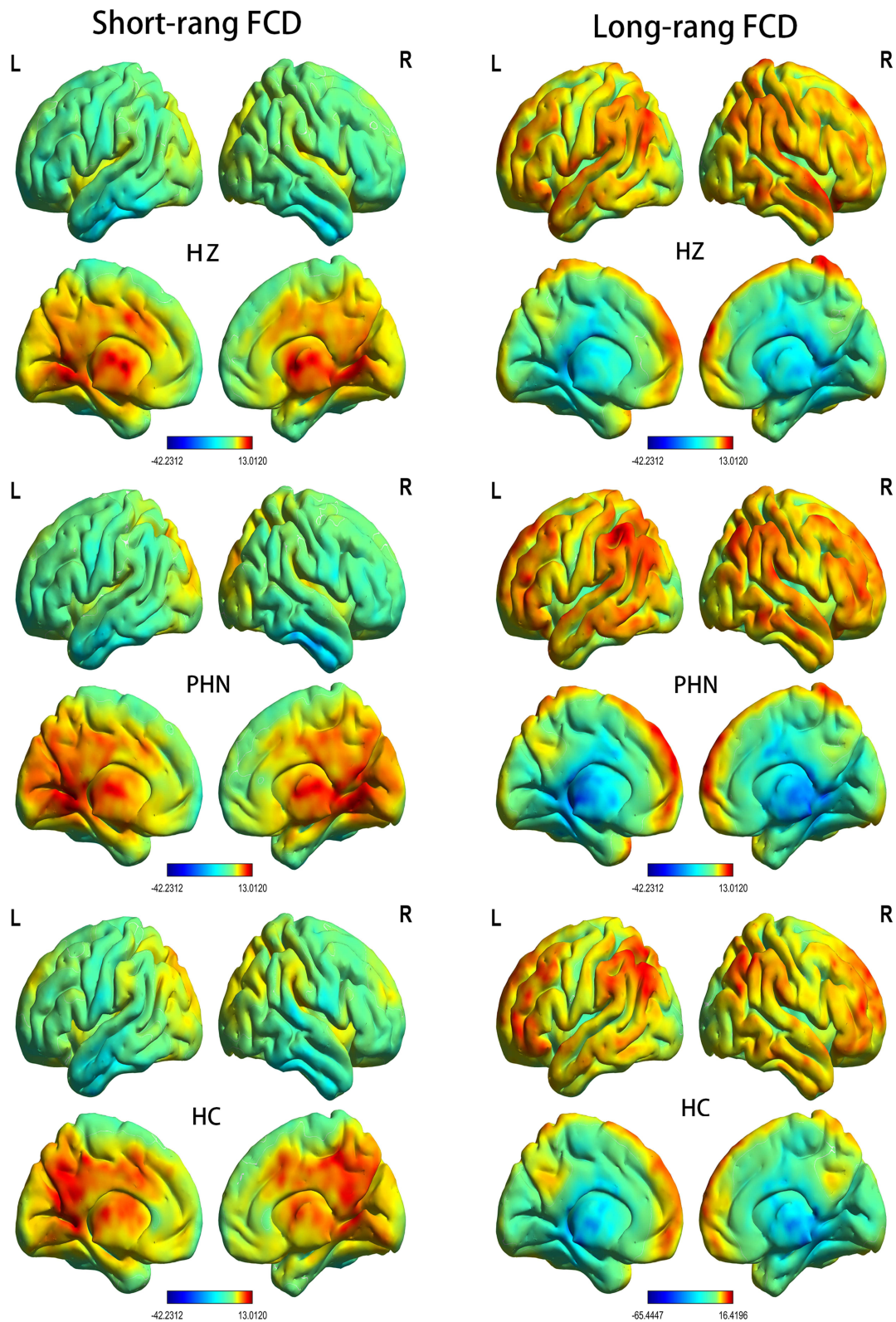
Figure 1 Spatial distribution of short-range and long-range FCD in the HZ, PHN, and HC groups.

values were higher in the anterior cingulate and cingulate gyrus, and long-range FCD values were higher in the postcentral gyrus, precentral gyrus, and frontal lobe.

Differences in Short-Range FCD and Long-Range FCD Among the HZ, PHN, and HC Groups

Compared with the HC group, the HZ group exhibited a significant increase in long-range FCD of the bilateral cerebellum, thalamus (THA), parahippocampal gyrus (PHG), superior temporal gyrus (TPOsup), and right lingual gyrus (LING) as well as a significant decrease in the short-range FCD of the bilateral posterior cingulate gyrus (PCG), median cingulate and paracingulate gyri (DCG), and left precuneus (PCUN) (Figure 2 and Table 2). Compared with the HC group, the PHN group exhibited a significant decrease in the long-range FCD of the bilateral superior frontal gyrus (SFG) as well as a significant decrease in the short-range FCD of the bilateral PCG, DCG, and PCUN (Figure 3 and Table 3). However, there were no significant differences between the PHN and the HZ groups in either long- or short-range FCD.

Seed-Based Whole-Brain rsFC Analysis

We defined the regions showing differences in long-range FCD values as ROIs between the HZ and PHN groups and examined the functional connections of these regions with the whole brain. In the PHN group, the rsFC of the bilateral SFG showed significant differences (Figure 4), and the FC between the bilateral SFG and right insula in PHN patients was significantly increased (Figure 4 and Table 4). However, compared with the HC group, the HZ group did not exhibit significant differences in rsFC between regions with changes in long-range FCD and the whole brain.
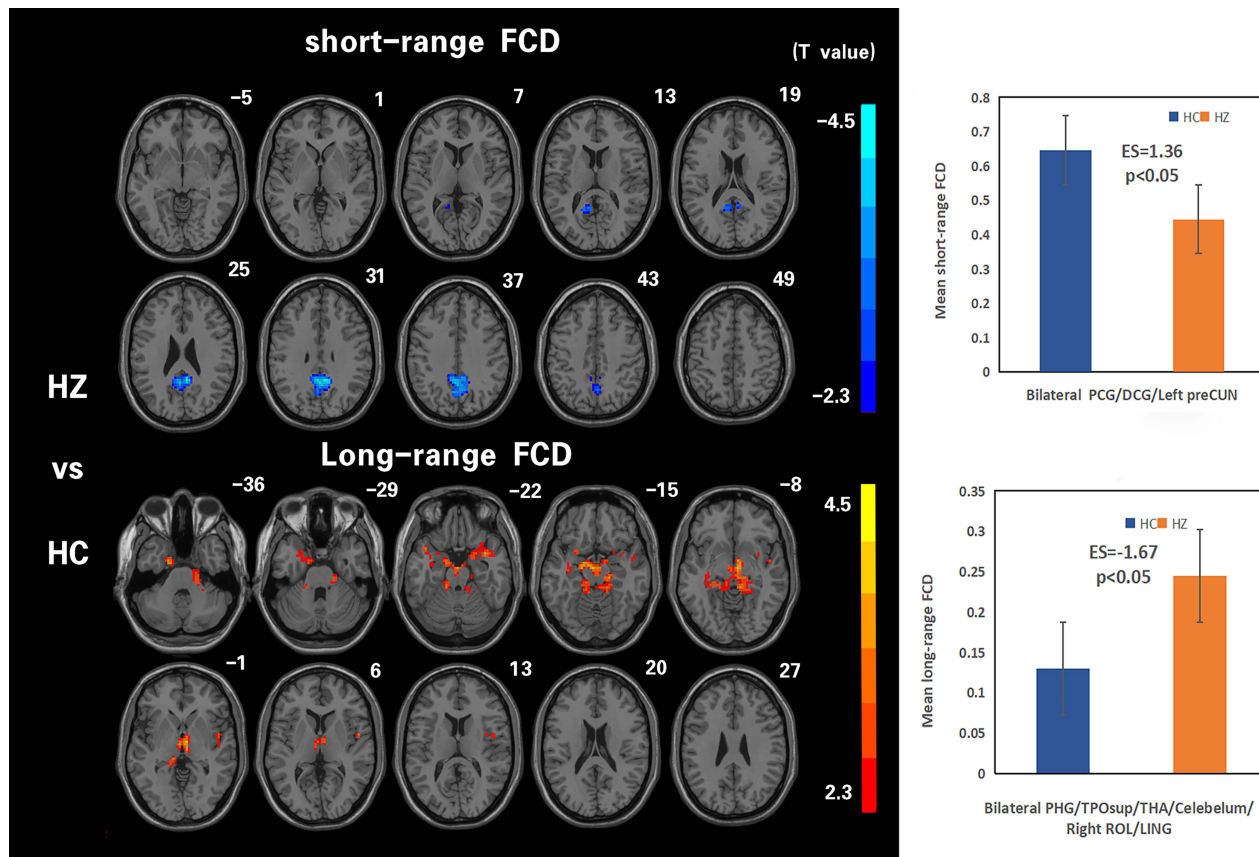
Figure 2 Distribution of brain areas with inter-group differences in short-range and long-range FCD between the HZ group and HC group (GRF corrected, voxel-level P<0.01, cluster-level P<0.05) and comparison of average short-range and long-range FCD in brain regions that differed between the HZ group and HC group (P<0.05).

Table 2 Differences in Short-Range FCD and Long-Range FCD Between HZ Group and HC Group (GRF Corrected, Voxel Level P<0.01, Cluster Level P<0.05)

Brain regions	Cluster Size (Voxels)	MNI Coordinates			F Values	ES
		x	y	z		
Decreased short-range FCD						
Bilateral PCG/DCG/Left PCUN	444	6	−48	27	−4.4163	1.3651
Increased long-range FCD						
Bilateral cerebellum/THA/PHG/TPOsup/LING	1089	6	−12	−3	4.4276	−1.6779

Notes: A positive F value indicates that the resting-state FCD value of the HZ group was greater than that of the HC group; a negative F value indicates that the resting-state FCD value of the HZ group was less than that of the HC group.
**Abbreviations**: FCD, functional connectivity density; HZ, herpes zoster; HC, healthy control; ES, effect size.

Correlations of Brain Regions with Inter-Group Differences in FCD and rsFC with Clinical Data

Long-range FCD values in the bilateral SFG were correlated with pain duration in the PHN group (r=−0.58, P=0.011) (Figure 5). However, no significant correlations were observed between the FCD and rsFC values and other clinical variables.

Receiver Operating Characteristic (ROC) Analysis of FCD in the Altered Regions Between the Groups

As mentioned above, bilateral cerebellum/THA/PHG/TPOsup/LING showed significantly different long-range FCD between the HZ and HCs, and bilateral SFG showed significantly different long-range FCD between the PHN and
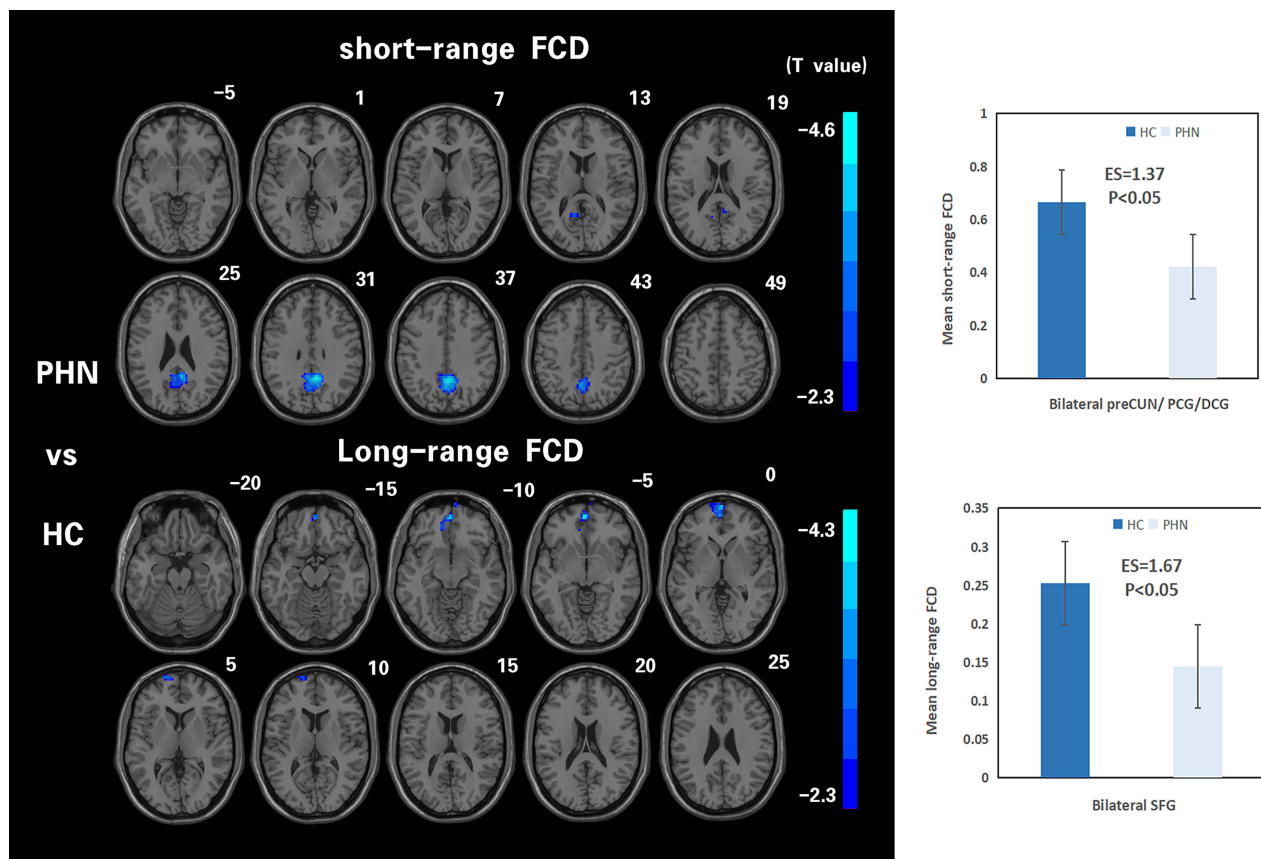
Figure 3 Distribution of brain areas with inter-group differences in short-range and long-range FCD between the PHN group and HC group (GRF corrected, voxel-level P<0.01, cluster-level P<0.05) and comparison of average short-range and long-range FCD in brain areas that differed between the PHN group and HC group (P<0.05).

Table 3 Differences in Short-Range FCD and Long-Range FCD Between PHN Group and HC Group (GRF Corrected, Voxel Level P<0.01, Cluster Level P<0.05)

Brain regions	Cluster Size (Voxels)	MNI Coordinates			F Values	ES
		x	y	z		
Decreased short-range FCD						
Bilateral PCG/DCG/PCUN	418	0	−54	36	−4.5949	1.3711
Decreased long-range FCD						
Bilateral SFG	517	−3	57	−3	−4.2359	1.6779

Notes: A negative F value indicates that the resting-state FCD value of the PHN group was less than that of the HC group.
Abbreviations: FCD, functional connectivity density; PHN, postherpetic neuralgia; HC, healthy control; ES, effect size.

HCs, suggesting that the long-range FCD in these brain regions can be used to discriminate between HZ and HCs as well as PHN and HCs. To investigate this possibility, the mean long-range FCD values in these regions were extracted, and ROC analysis was conducted. Areas under the curves of the two regions were 0.887 for the bilateral cerebellum/THA/PHG/TPOsup/LING (Figure 6) and 0.957 for the bilateral SFG (Figure 7).

Discussion
Differences in FCD Among the HZ, PHN, and HC Groups

This study used FCD to investigate alterations in spontaneous brain activity in patients with HZ and PHN. Furthermore, We differentiated between short- and long-range FCD to explore changes in intra- and inter-regional functional connectivity in these patients. Compared with those of the HC group, the HZ and PHN groups exhibited significant decreases in the short-range FCD of the PCG, DCG, and precuneus.

The DCG and PCG comprise the cingulate cortex, which is involved in the subjective perception of pain and its cognitive and emotional regulation.[15] In a study on chronic pain,[16] a high concentration of opiate receptor binding sites was observed in the cingulate cortex, suggesting that the DCG and PCG play important roles in the formation and modulation of pain. The default mode network (DMN) is a functional brain network that typically exhibits stronger activity at rest than during task execution, especially the execution of cognitive tasks, when its spontaneous activity is somewhat suppressed.[17] The cingulate cortex/precuneus is a core node of the DMN, playing a pivotal role in information transmission, and is significantly associated with the processing of various sensory information.[7] We detected a decrease
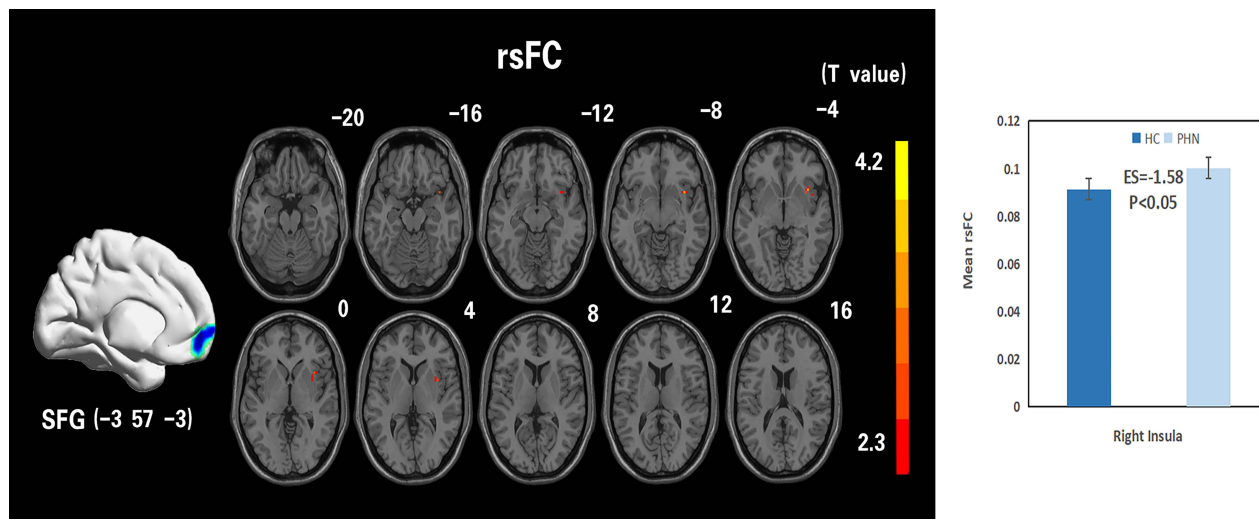
Figure 4 Distribution of brain areas with differences in the rsFC of ROIs between the PHN group and HC group (GRF corrected, voxel-level P<0.01, cluster-level P<0.05) and comparison of the average rsFC in brain areas that differed between the PHN group and HC group (P<0.05).

Table 4 Brain Regions with Abnormal rsFC in PHN Group Based on ROI (GRF Corrected, Voxel Level P<0.01, Cluster Level P<0.05)

| Brain regions	Cluster Size (Voxels)	MNI Coordinates			T Values	ES
		x	y	z		
ROI: Bilateral SFG Regions with Increased rsFC: Right insula	25	36	12	−9	4.1564	−1.5882

Notes: A positive T value indicates that the resting-state FC value of the PHN group was greater than that of the HC group.
Abbreviations: rsFC, resting-state functional connectivity; PHN, postherpetic neuralgia; HC, healthy control; ES, effect size.

in the short-range FCD of the PCG, DCG, and precuneus in HZ and PHN patients, which is consistent with previous research,[10] indicating that pain due to HZ and PHN may disrupt the DMN and that impairment of the DMN can occur as early as the acute phase of herpes zoster.

Furthermore, compared to the HC group, the HZ patients exhibited a significant increase in the long-range FCD of different brain regions, including the cerebellum, thalamus, parahippocampal gyrus, superior temporal gyrus, and lingual gyrus. Among these regions, the cerebellum and thalamus are both pain-related areas and part of the "pain matrix", which is defined as areas reliably activated in response to increasing levels of pain.[18] The cerebellum projects to the thalamus, transmitting a variety of information that subsequently ascends to the cerebral cortex, and the cerebral cortex sends this information back to the cerebellum via the pons and inferior olive.[19] The input of various pain-related information into the cerebellum suggests that it is a crucial center for processing pain information. The thalamus is a vital sensory hub and an important information integration center for pain processing, playing a key role in regulating and mediating cortical excitability in response to pain signals.[20] Therefore, it was anticipated that the long-range FCD of the cerebellum and thalamus would significantly increase in HZ patients. Pain is known to be a complex sensation encompassing sensory, affective, and cognitive dimensions.[21] The parahippocampal gyrus is part of the limbic system and is closely related to emotion regulation. We found an increase in the long-range FCD of the parahippocampal gyrus in HZ patients, indicating that the limbic system and the pain matrix both participated in the regulation of complex neuropathic pain. Our study results suggest that the superior temporal gyrus and lingual gyrus were involved, in addition to pain-related areas and the
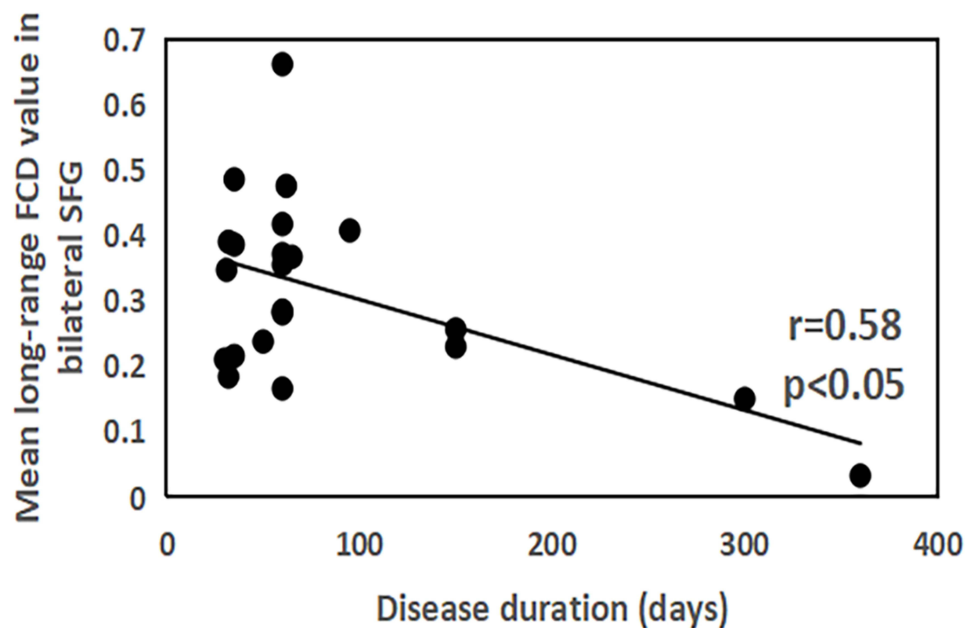
Figure 5 Correlation between FCD values in brain regions with inter-group differences and clinical data.
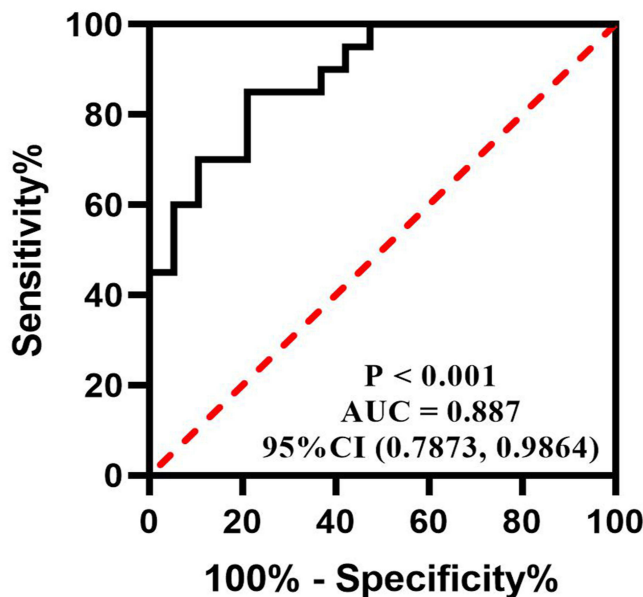
Figure 6 ROC analysis of long-range FCD in the altered regions as a potential means to differentiate between patients with HZ and healthy subjects.
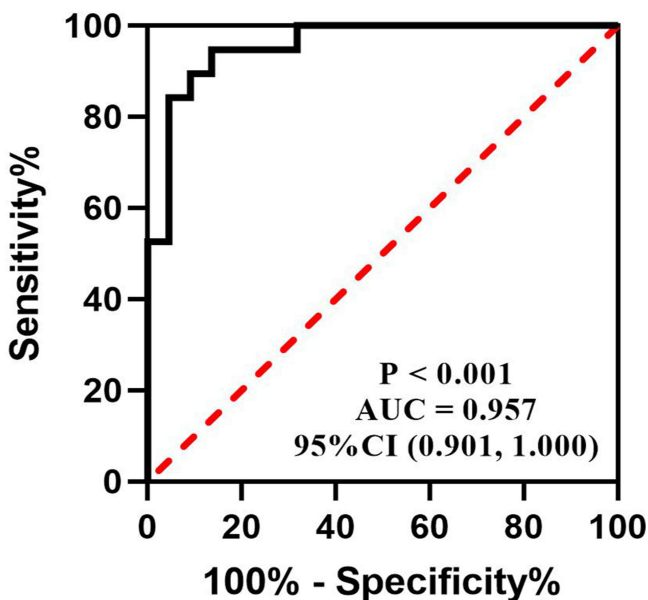

Figure 7 ROC analysis of long-range FCD in the altered regions as a potential means to differentiate between patients with PHN and healthy subjects.

limbic system. The superior temporal gyrus is a part of the auditory language center that plays a crucial role in language comprehension, auditory processing, and visual search.[22] The lingual gyrus is an important area for processing visual information. However, to date, there have been no reports of visual or auditory abnormalities in patients with HZ, and it is unclear whether these abnormal changes are potentially related to the disease.

We discovered alterations in intra- and inter-regional functional connectivity in HZ and PHN patients; however, no significant differences in short- or long-range FCD were found between the PHN and HZ groups. We believe that this is attributed to the use of stringent statistical methods in inter-group comparisons; additionally, the duration of PHN was relatively short in this study. Therefore, in future research, we will endeavor to expand the sample size and recruit these patients with longer disease duration.

Alterations in Seed-Based rsFC are Associated with Differences in Long-Range FCD in the PHN Group

Long-range FCD of the bilateral SFG decreased in patients with PHN. The SFG is located in the upper region of the frontal cortex and is responsible for working memory, stress perception, and the regulation of aversive emotions.[23] The frontal cortex is vital for cognitive control and plays a crucial role in the pain/emotion regulation pathway. It is involved in the processing and integrating emotional information and regulating the direction and intensity of emotional responses.[24] Prior researches have established the involvement of prefrontal cortices (eg, IFG, MFG, SFG) in pain's affective and cognitive dimensions.[25,26] The medial prefrontal cortex encodes the subjective perception of ongoing pain, and gamma oscillations in this region encode subjection pain perception.[27] SFG reportedly encodes subjective perception at the beginning and end of the tonic stimulus.[28] The prefrontal cortex receives ascending, nociceptive input and controls top-down pain. Thus, SFG plays an important role in the pain pathway. In addition, previous research has revealed close relationships of the frontal lobe with depression and anxiety[29] and has confirmed the associations of PHN with depression and anxiety.[30] We found significant differences in HAMA and HAMD scores between HZ and PHN patients ($P<0.05$), with more pronounced affective symptoms observed in PHN patients than in HZ patients, suggesting that long-range chronic pain in PHN patients may impair the pain/emotion regulation pathway, thereby resulting in poorer emotion regulation abilities.

Further seed-based rsFC analysis showed a significant increase in FC between the bilateral SFG and the right insula. The insula is strongly associated with pain perception. The posterior insula receives sensory input from the somatosensory cortex and the ventroposterolateral thalamic nucleus, encoding the pain experience, In contrast, the anterior insula connects with the limbic system and frontal cortex, playing a role in evaluating pain intensity.[31,32] In chronic neuropathic pain, metabolic changes such as an increase in the choline concentration and upregulation of M2 muscarinic receptors in the posterior insula have been observed.[33] The enhanced functional activity of the insula in PHN patients may be related to the activation of M2 muscarinic receptors expressed in the insula. The projections from the insular cortex to the bilateral frontal cortex can activate the pathway for evaluating pain intensity.[34] In addition, the long-range FCD values of the bilateral SFG were negatively correlated with the duration of pain in the PHN group. The SFG encodes the subjective perception of ongoing pain and plays a crucial part role of in the pain/emotion regulation pathway.[23,26] This suggests that long-range transmission of pain information alters the endogenous analgesia mechanism in patients with PHN, modifies the affective response to pain, or decrease the subjective perception of pain and associated cognition to reduce the input of pain signals. This may be an adaptive mechanism of the brain's processing of pain information after long-term pain.

Receiver Operating Characteristic (ROC) Analysis of FCD in the Altered Regions Between the Groups

The long-range FCD in bilateral cerebellum/THA/PHG/TPOsup/LING can be used to discriminate between HZ and HCs. The long-range FCD in bilateral SFG can be used to distinguish PHN and HCs. Therefore, bilateral cerebellum/THA/PHG/TPOsup/LING and bilateral SFG may be specific neuroimaging markers of HZ and PHN. Based on this, in the future, these special neuroimaging markers can be validated through deep learning methods, which will help in the early diagnosis of HZ and PHN.

Limitations

Our study had certain limitations. First, the duration of PHN was relatively short (average, 85.5 days). Second, each patient had varying severity and location of skin damage, and whether these differences would lead to changes in brain functional connectivity requires further exploration. Third, the sample size of this study was small. In subsequent studies, we aim to increase the sample size to replicate the results of a study with large samples.

Conclusion

This study found that the DMN was disrupted in HZ and PHN patients. Additionally, both the pain matrix and limbic system were found to participate in the regulation of complex neuropathic pain in HZ patients. However, long-term

chronic pain in PHN patients may impair the pain/emotion regulation pathway. Additionally, the long-range transmission of pain information may adjust the endogenous analgesia mechanism in PHN patients, causing abnormalities in local brain activity in the areas responsible for emotion regulation and pain modulation.

Funding

Disclosure

The authors report no conflicts of interest in this work.

References

1. Warner BE, Goins WF, Kramer PR, Kinchington PR. A guide to preclinical models of zoster-associated pain and postherpetic neuralgia. *Curr Top Microbiol Immunol*. 2023;438:189–221. doi:10.1007/82_2021_240
2. Bianchi L, Piergiovanni C, Marietti R, et al. Effectiveness and safety of lidocaine patch 5% to treat herpes zoster acute neuralgia and to prevent postherpetic neuralgia. *Dermatol Ther*. 2021;34(1):e14590. doi:10.1111/dth.14590
3. Ou M, Chen J, Yang S, Xiao L, Xiong D, Wu S. Rodent models of postherpetic neuralgia: how far have we reached? *Front Immunol*. 2023;14:1026269. doi:10.3389/fimmu.2023.1026269
4. Gauthier A, Breuer J, Carrington D, Martin M, Rémy V. Epidemiology and cost of herpes zoster and post-herpetic neuralgia in the United Kingdom. *Epidemiol Infect*. 2009;137(1):38–47. doi:10.1017/S0950268808000678
5. Cao S, Li Y, Deng W, et al. Local brain activity differences between herpes zoster and postherpetic neuralgia patients: a resting-state functional MRI study. *Pain Physician*. 2017;20(5):E687–E699.
6. Jiang J, Gu L, Bao D, et al. Altered homotopic connectivity in postherpetic neuralgia: a resting state fMRI study. *J Pain Res*. 2016;9:877–886. doi:10.2147/JPR.S117787
7. T D, Nd V. Functional connectivity density mapping. *Proc Natl Acad Sci USA*. 2010;107(21). doi:10.1073/pnas.1001414107
8. Tomasi D, Volkow ND. Aging and functional brain networks. *Mol Psychiatry*. 2012;17(5):471, 549–558. doi:10.1038/mp.2011.81
9. Martínez-Molina N, Siponkoski ST, Kuusela L, et al. Resting-state network plasticity induced by music therapy after traumatic brain injury. *Neural Plast*. 2021;2021:6682471. doi:10.1155/2021/6682471
10. Hong S, Gu L, Zhou F, et al. Altered functional connectivity density in patients with herpes zoster and postherpetic neuralgia. *J Pain Res*. 2018;11:881–888. doi:10.2147/JPR.S154314
11. Lv H, Wang Z, Tong E, et al. Resting-state functional MRI: everything that nonexperts have always wanted to know. *AJNR Am J Neuroradiol*. 2018;39(8):1390–1399. doi:10.3174/ajnr.A5527
12. Merskey H, Bogduk N, Peralta E. Classification of chronic pain: descriptions of chronic pain syndromes and definitions of pain terms. *Pain*. 1994;56(1):3. doi:10.1016/0304-3959(94)90144-9
13. Mao Y, Liao Z, Liu X, et al. Disrupted balance of long and short-range functional connectivity density in Alzheimer's disease (AD) and mild cognitive impairment (MCI) patients: a resting-state fMRI study. *Ann Transl Med*. 2021;9(1):65. doi:10.21037/atm-20-7019
14. Mégevand P, Groppe DM, Goldfinger MS, et al. Seeing scenes: topographic visual hallucinations evoked by direct electrical stimulation of the parahippocampal place area. *J Neurosci*. 2014;34(16):5399–5405. doi:10.1523/JNEUROSCI.5202-13.2014
15. Rolls ET. The cingulate cortex and limbic systems for action, emotion, and memory. *Handb Clin Neurol*. 2019;166:23–37. doi:10.1016/B978-0-444-64196-0.00002-9
16. Liu H, Liu Z, Liang M, et al. Decreased regional homogeneity in schizophrenia: a resting state functional magnetic resonance imaging study. *Neuroreport*. 2006;17(1):19–22. doi:10.1097/01.wnr.0000195666.22714.35
17. Smallwood J, Bernhardt BC, Leech R, Bzdok D, Jefferies E, Margulies DS. The default mode network in cognition: a topographical perspective. *Nat Rev Neurosci*. 2021;22(8):503–513. doi:10.1038/s41583-021-00474-4
18. Garcia-Larrea L, Peyron R. Pain matrices and neuropathic pain matrices: a review. *Pain*. 2013;154(Suppl 1):S29–S43. doi:10.1016/j.pain.2013.09.001
19. Moulton EA, Schmahmann JD, Becerra L, Borsook D. The cerebellum and pain: passive integrator or active participator? *Brain Res Rev*. 2010;65 (1):14–27. doi:10.1016/j.brainresrev.2010.05.005
20. Yosten GL, Harada CM, Haddock C, et al. GPR160 de-orphanization reveals critical roles in neuropathic pain in rodents. *J Clin Invest*. 2020;130 (5):2587–2592. doi:10.1172/JCI133270
21. Malfliet A, Coppieters I, Van Wilgen P, et al. Brain changes associated with cognitive and emotional factors in chronic pain: a systematic review. *Eur J Pain*. 2017;21(5):769–786. doi:10.1002/ejp.1003
22. Sjk S, J R, S S, et al. Intracranial recordings demonstrate both cortical and medial temporal lobe engagement in visual search in humans. *J Cognitive Neurosci*. 2021;33(9). doi:10.1162/jocn_a_01739
23. Jones DT, Graff-Radford J. Executive dysfunction and the prefrontal cortex. *Continuum (Minneap Minn)*. 2021;27(6):1586–1601. doi:10.1212/CON.0000000000001009

24. Li J, Huang X, Sang K, Bodner M, Ma K, Dong XW. Modulation of prefrontal connectivity in postherpetic neuralgia patients with chronic pain: a resting-state functional magnetic resonance-imaging study. *J Pain Res*. 2018;11:2131–2144. doi:10.2147/JPR.S166571

25. Kucyi A, Davis KD. The dynamic pain connectome. *Trends Neurosci*. 2015;38(2):86–95. doi:10.1016/j.tins.2014.11.006

26. Bastuji H, Frot M, Perchet C, Magnin M, Garcia-Larrea L. Pain networks from the inside: spatiotemporal analysis of brain responses leading from nociception to conscious perception. *Hum Brain Mapp*. 2016;37(12):4301–4315. doi:10.1002/hbm.23310

27. Schulz E, May ES, Postorino M, et al. Prefrontal gamma oscillations encode tonic pain in humans. *Cereb Cortex*. 2015;25(11):4407–4414. doi:10.1093/cercor/bhv043

28. Caston RM, Davis TS, Smith EH, Rahimpour S, Rolston JD. A novel thermoelectric device integrated with a psychophysical paradigm to study pain processing in human subjects. *J Neurosci Methods*. 2023;386:109780. doi:10.1016/j.jneumeth.2022.109780

29. Vialou V, Bagot RC, Cahill ME, et al. Prefrontal cortical circuit for depression- and anxiety-related behaviors mediated by cholecystokinin: role of ΔFosB. *J Neurosci*. 2014;34(11):3878–3887. doi:10.1523/JNEUROSCI.1787-13.2014

30. Denkinger MD, Lukas A, Nikolaus T, Peter R, Franke S. ActiFE study group. multisite pain, pain frequency and pain severity are associated with depression in older adults: results from the ActiFE Ulm study. *Age Ageing*. 2014;43(4):510–514. doi:10.1093/ageing/afu013

31. Kong J, White NS, Kwong KK, et al. Using fMRI to dissociate sensory encoding from cognitive evaluation of heat pain intensity. *Hum Brain Mapp*. 2006;27(9):715–721. doi:10.1002/hbm.20213

32. Tran The J. The role of structural and functional insular cortex abnormalities in body perception disturbance in schizophrenia. *Encephale*. 2021;47 (3):270–276. doi:10.1016/j.encep.2020.11.004

33. Ferrier J, Bayet-Robert M, Dalmann R, et al. Cholinergic neurotransmission in the posterior insular cortex is altered in preclinical models of neuropathic pain: key role of muscarinic M2 receptors in donepezil-induced antinociception. *J Neurosci*. 2015;35(50):16418–16430. doi:10.1523/JNEUROSCI.1537-15.2015

34. Oshiro Y, Quevedo AS, McHaffie JG, Kraft RA, Coghill RC. Brain mechanisms supporting discrimination of sensory features of pain: a new model. *J Neurosci*. 2009;29(47):14924–14931. doi:10.1523/JNEUROSCI.5538-08.2009